Estimation of the Best fit Rainfall-Runoff Relationship for the Upper Blue Nile Basin

Assem Afify [1], Dr. Kamal Hefny [2], Dr. Mohamed Elmotasem [3], and Dr. Abdelatef Mehana [4]

[1] Research professor, National Water Research Center, P.O. Box 6, 13621 Qalubia, Egypt.
[2] Emeritus professor, National Water Research Center, P.O. Box 6, 13621 Qalubia, Egypt.
[3] Emeritus professor, National Water Research Center, P.O. Box 6, 13621 Qalubia, Egypt.
[4] Former Director of research, Egyptian Meteorological Authority, Cairo, Egypt.

Abstract

The Blue Nile water is the main source of the Nile River, which contributes approximately 60% of the Nile River flow arriving at Aswan Dam, Egypt. Rainfall-runoff relationships were obtained to predict the stream flow at the shed outlet using both simple linear and nonlinear regression models. Meteorological records (1908-2007) for the total monthly rainfall of representative 33 NOAA' stations were used along with hydrological data series (1966-2005) for the gauge outflow at El-Deim. Last eight years of rainfall and stream flow records were used for the validation of the obtained rainfall-runoff relations. Monthly runoff coefficients were estimated with an overall average of 20%. The best fit rainfall-runoff relations with two trends (rising and falling stage) were observed and presented in the paper.

Keywords: Blue Nile, climate, forecasting, hydrology, hysteresis, rainfall, regression models, and runoff coefficient.

1. INTRODUCTION

As reported by the World Development figures (WDS, 2014), Egypt has reached the water poverty threshold of less than 1000 m^3/capita/year, where current per capita annual water share is about 600 m3. It is estimated that Ethiopia has a per capita water availability of 1900 m^3/capita/year (Negash, 2012). The Blue Nile Basin is the main source of the Nile River with a drainage area of 324,530 km^2 (Peggy and Curtis, 1994). The Upper Blue Nile basin has an area of 172,250 km^2, which contributes approximately 60% of the Nile River flow at Aswan Dam, Egypt (IPoE, 2013). Based on flood frequency analysis studies (DICAM, 2011), The Upper Blue Nile basin receives an average of 1,300 mm of precipitation annually. Year-to-year variations are considerable, ranging from 1050 mm to more than 1550 mm across the historical record (King, 2013).

In a study for the climate and hydrology of the upper Blue Nile River, Conway (2000) reported a mean annual basin rainfall of 1421 mm based on 11 gauges for the period 1900-1998, with about 70% occurring between June and September. Moreover, he reported that rainfall over the basin showed a marked decrease between the mid- 1960s and the late 1980s. Characteristics of the mo-nthly and annual rainfall of the basin were investigated by Abtew et. Al (2008). Based on normal distribution data-fitting, the 100-year drought annual basin rainfall was estimated as 1132 mm, while the 100-year wet annual rainfall was 1745 mm. The wet season runs from June through September and the dry season is from November through April; October and May are transitional months (Abtew et. Al, 2008).

An appraisal study was presented by Bashar et. Al (2006) to select a suitable model(s), that can be used in forecasting river flows of the Nile basin. In this appraisal study, systems and conceptual modeling techniques (such as the simple linear model, the linear perturbation model, and the Artificial Neural Network Model) were applied to Lake Victoria catchments, Awash and the Blue Nile catchment up to Eddeim of the Ethiopian high lands. The models were applied in non-parametric and parametric forms. Parameter optimization was carried out by ordinary least squares, Rosenbrock, Simplex and genetic algorithm.

It was shown that the simple assumption of linearity was not adequate in modelling the rainfall runoff transformation. However, in catchments which exhibit marked seasonal behaviour good results can be obtained with Linear Perturbation Model (LPM) which involves the assumption of linearity between the departures from seasonal expectations in input and output series (Bashar et. Al, 2006).

Long-term simulations were performed by Elshamy (2008) for the purpose of the assessment of the performance of the Nile Forecast System (NFS) hydrological component addressing climate change impacts on the river flow. The assessment used available daily and monthly rainfall and runoff data within the NFS database for the period 1940-1999. Simulated monthly flow series were compared to observations at the Blue Nile as one of seven key locations. The performance criteria measuring different aspects of flow were calculated for the monthly series. The best fit R^2 of 0.79 was achieved for the Blue Nile (Elshamy, 2008).

The main goal of the current study is the prediction of the monthly runoff volume at the shed outlet for the upper Blue Nile (Abbay) basin. Specifically, the study objectives are outlined to obtain the best fit rainfall-runoff relations and estimation of the stream flow at the shed outlet, and consequently obtain the monthly runoff coefficients for the basin.

Definitions:
Hysteresis is the dependence of the output of a system not only on its current input, but also on its history of past inputs. The dependence arises because the history affects the value of an internal state. If a given input alternately increases and decreases, a typical mark of hysteresis is that the output forms a loop. Such loops may occur purely because of a dynamic lag between input and output.
Lag-time in this paper is the delay time between the output (stream flow) and the input (rainfall).

2. DATA COLLECTION

Intensive meteorological and hydrological data were collected for the Abbay water shed trying to reach or find out a relationship between the total monthly rainfall and gauged stream flow at the shed outlet. In what follows, a brief description is given for both meteorological and hydrological data collected.

2.1. Meteorological Data: Monthly rainfall data was reviewed for about 123 NOAA' stations covering the whole Ethiopian plateau including the Blue Nile. Later on, these stations were screened to come up with a number of 33 stations (Table 1) within the upper Blue Nile (Abbay) watershed. Figure 1 shows the locations of these stations representing the Abbay water shed. Rainfall records (1908-2007) for the total monthly rainfall were obtained via electronic download from NOAA's Web site. Figure 2 represents climatic average for rainfall hydrographs (over a period of time) for six significant stations having at least 30 years of continuous records.

It is obvious from figure 2 that significant rainfall starts in April, increases gradually to reach the peak in July and August, and then decreases until November. The dry period from December through March was not taken into consideration in the current study. The mean annual rainfall excluding dry months was found to be 1240 mm over the study period. As shown in Figure 1, the distribution of the rainfall gauge stations covers the whole catchment boundary, and well represents the different catchment topography; as well as soil types, land cover, and land use for the whole catchment.

2.2. Hydrological data: Moreover, the stream flow gauge station at El-Deim (Figure 1) is representing the shed outlet (25 Km to the upstream from the Ethiopian border). Data for this station were obtained from the Nile Sector (NCD, 2000). Since El-Deim station was not established before 1966, El-Deim records (1966–1997) were used in the current research for the analysis to represent the stream flow at the Abbay shed outlet.

Records (1966–2005) for the total monthly flow at El-Deim station were analyzed. The flow hydrograph for El-Deim station was presented as shown in Figure 3, showing the peak monthly flow in August. The main observation from the previous data summary is that the peak monthly flow in August, while the peak monthly rainfall is mostly in July.

Table 1: Names of selected rain gauges in the Abbay river basin

No.	Name	No.	Name	No.	Name	No.	Name
1	Gondar	10	Maksegnit	19	Dangla	28	Shambo
2	Bahr Dar	11	Limu Genet	20	Muja	29	Anger Gutin
3	Combolcha	12	Harar Meda	21	Kemise	30	Mendi
4	Debre Marcos	13	Gorgora	22	Kule Mesk	31	Sekoru
5	Assossa	14	Ebnat	23	Cheffe	32	Ghion Police St.
6	Nekemete	15	Zege	24	Fincha' Adam	33	Ameya Gindo
7	Addis Ababa	16	Debre Tabor	25	Dejen		
8	Sibu Sire	17	Mandura	26	Arjo		
9	Debat	18	Chagni	27	Haro		

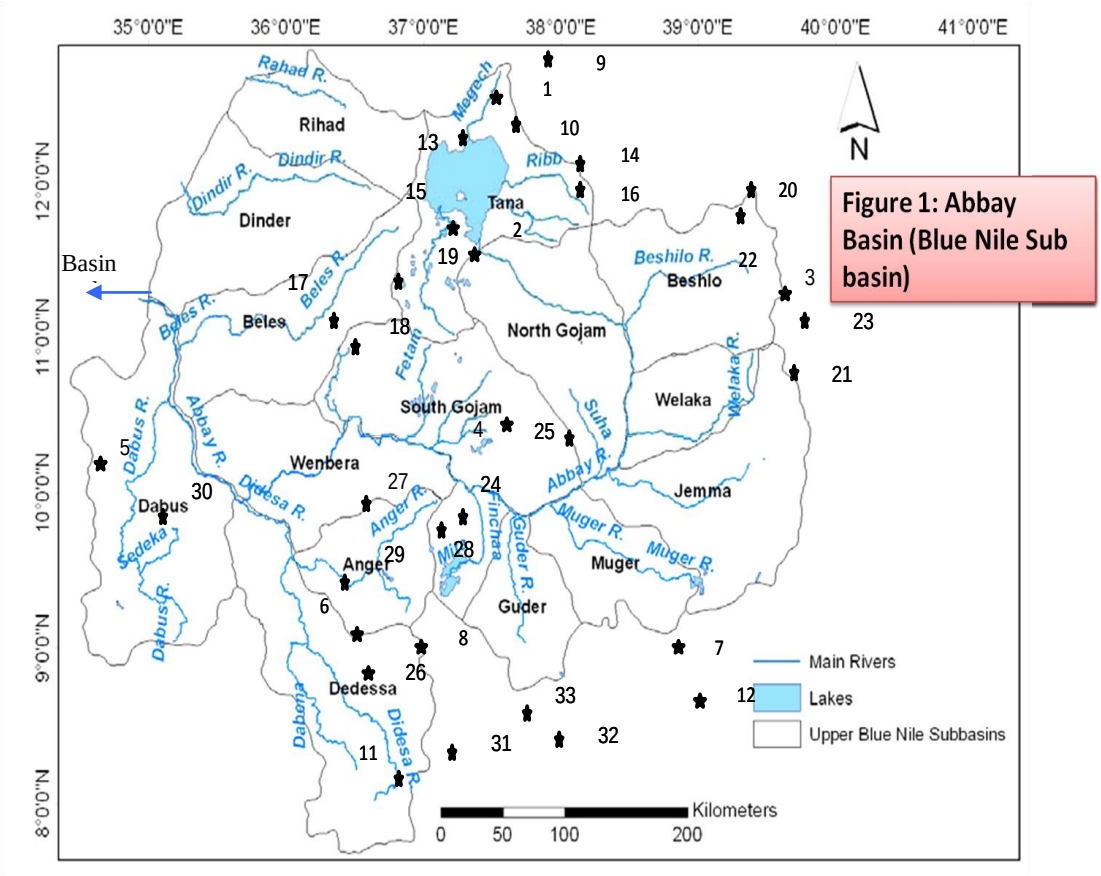

Figure 1: Upper Blue Nile river basin (Abbay) and the locations of selected rainfall gauge stations

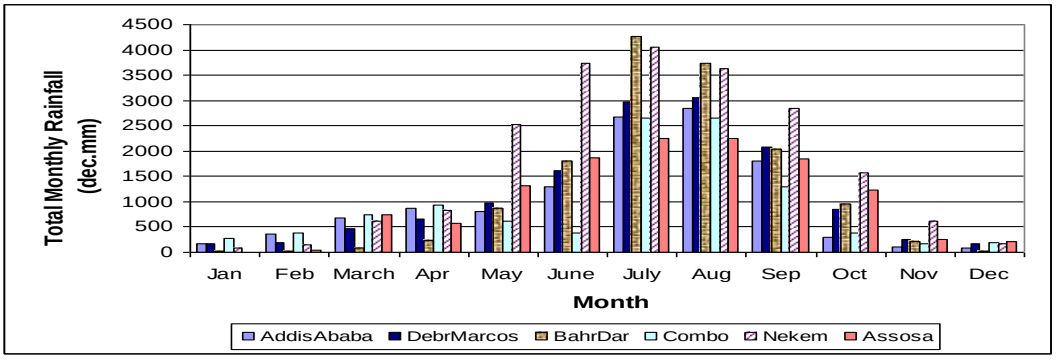

Figure 2: Climatic average total monthly rainfall for significant stations in the Abbay basin.

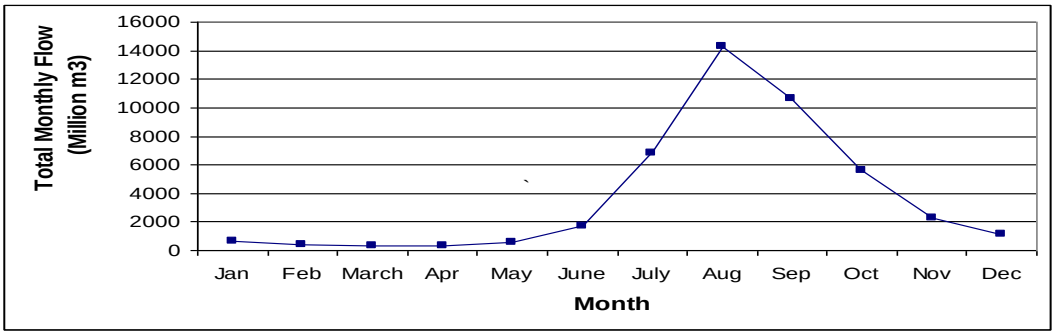

Figure 3: Mean total monthly flows for El-Deim (1966-1997)

3. METHODOLOGY

The analysis of the collected data has passed through fulfilling the following steps:

1. Locating 33 out of 123 NOAA' stations within the Abbay Basin.
2. Summarizing rainfall data for all 33 stations during a long period of records (1908-2007) in spread sheet format.
3. Summarizing total monthly stream flow records available for El-Diem station in spread sheet format.
4. Selection of El-Deim records (1966-2005), which is a good representation for the shed outlet and also has available data for at least seven rainfall stations.
5. Obtain the climatic averages for the total monthly rainfall; calculated as the arithmetic mean for all the representative stations during the selected calibration period (1966-1997), and plot it against the corresponding stream flow records. This estimation method using the arithmetic mean (Johnson, 1962) is simple and reliable for catchments with well spatially distributed and adequate number of 33 stations over the upper Blue Nile catchment.
6. Obtain rainfall-stream flow correlation coefficients on monthly basis, and during both of the rising period (April-August) and the recession period (August-November). Statistical functions built in Excell software have been used to obtain the correlations.
7. Using regression analysis, obtain the best fit relations between the total monthly rainfall and the total monthly stream flow for several cases considering both rising and recession period separately.
8. Verifications and validation of the best fit relation using the hidden data records kept from the entire records. The period 1998-2005 was selected for validation.
9. Obtain monthly stream flows from previous relations, and consequently obtain runoff coefficients on monthly basis.

4. DATA ANALYSIS AND RESULTS

Prior to the analysis of both meteorological and hydrological data, plotting of monthly stream flow against rainfall data was very helpful to get more insight and data visualization. This step was essential

to detect any outliers in both data sets and discard them appropriately. Figure 4a is an example of many scatter plots showing stream flow data against rainfall data for the month of September. Plots for other months and periods (rising and falling stages) are not illustrated in the text; however some of them will be shown appropriately later on. All these plots (Figures 4a, 4b, and 5) show direct proportional increase of stream flow against rainfall. This is an evident and logic result, which is also reflected from all the positive numbers, obtained for the rainfall-stream flow correlation coefficients (Table 2).

Scatter plot for all data points representing rainfall against runoff for the whole rainy season (April-November) is shown in figure 4b. Data points for the rising period "stage" (April-August) are well below all other data points for the falling stage (August-November). Moreover, the whole pattern of the scatter plot dictates a non-linear looping relationship (two trends); a hysteresis loop similar to the stage discharge relationship in hydrology (Wilson, 1983).

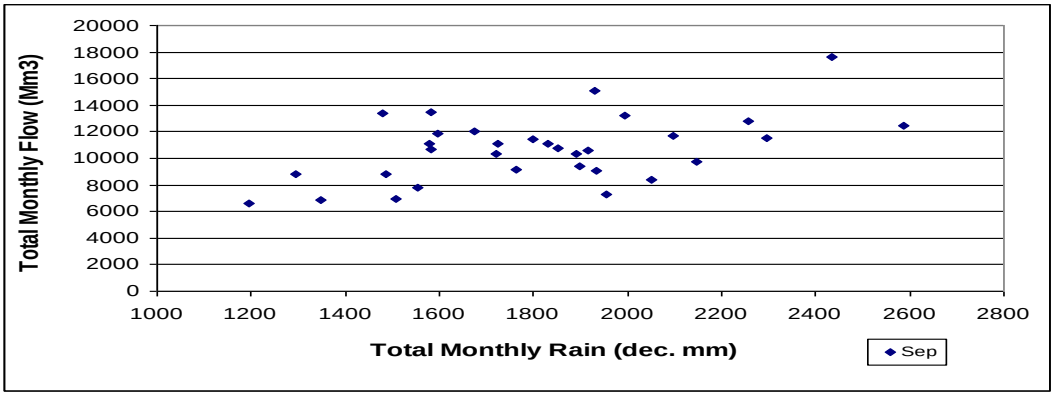

Figure 4a: Scatter plot showing rainfall data against stream flow data for September.

4.1. Correlation Results

Following step 6 in the methodology section, many trials have been performed for the rainfall-stream flow correlation analysis on monthly basis, and during the rainy season (April through November). Correlations were performed separately for both of the rising stage (April -August), and the recession stage (August-November) because of the looping phenomenon observed in figure 4b. The correlation coefficients (R) results are summarized in Table 2. From the table, it is shown that the monthly correlation coefficients are ranging from 0.47 to 0.67.

Correlation coefficients on monthly basis are slightly above 0.5, which are an indication to the scatter in the monthly data sets as shown in Figure 4a for September, as an example. However, the correlation coefficients are 0.81 and 0.92 for both of the rising and the falling periods, respectively. The higher correlation coefficients obtained for seasonal periods (rising and the falling) are very good indications to the physical hydrological phenomenon affected by the prior monthly rainfall data inputs. Therefore, it was concluded to obtain best fit relations based on the rising and falling periods rather than on monthly basis.

4.2. Regression Results

In this section the best-fit regression results for the rainfall-runoff relationship are illustrated for two distinct cases; the rising stage and the falling stage. Results for both of the rising stage and the falling stage are illustrated in the following paragraphs.

4.2.1. Rising stage: Figures 5 and 6 show the scatter plots results for the rising stage (April-August) with the best fit line added in figure 6. It is evident from the scatter shown by the figures that an exponential equation for the rainfall-runoff relationship can be drawn. Careful examination of the plot in figure 6 shows asymptotic to a minimal value, when the total monthly rainfall is approaching zero or no rainfall. The best fitting for the total monthly flow (F_t) versus the total monthly rainfall (R_t) is given in Equation (1) for the rising stage results.

$$F_t = 109.9e^{0.015\mathbf{R}}t \quad , R^2 = 0.895 \qquad \text{For rising stage (1)}$$

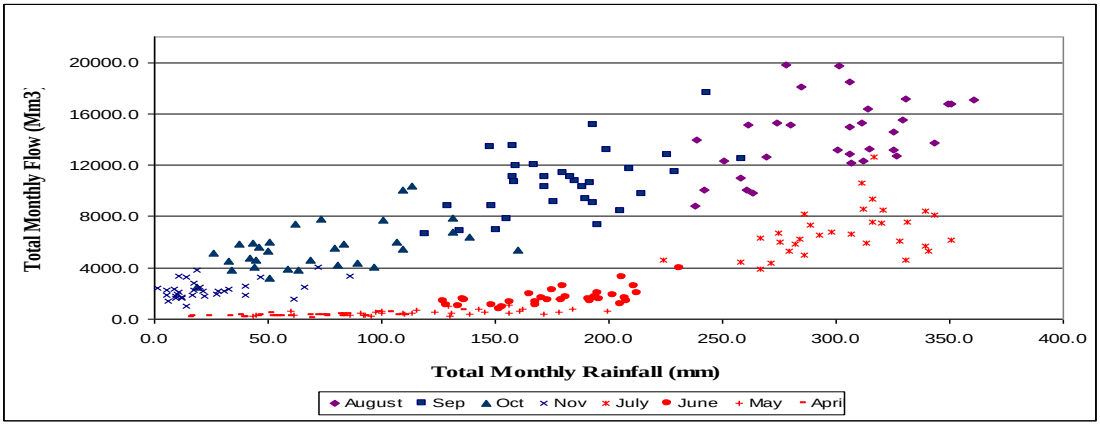

Figure 4b: Scatter plot for total monthly rainfall-runoff data, showing two trends for both of the rising (lower in red), and the falling stage (upper in blew).

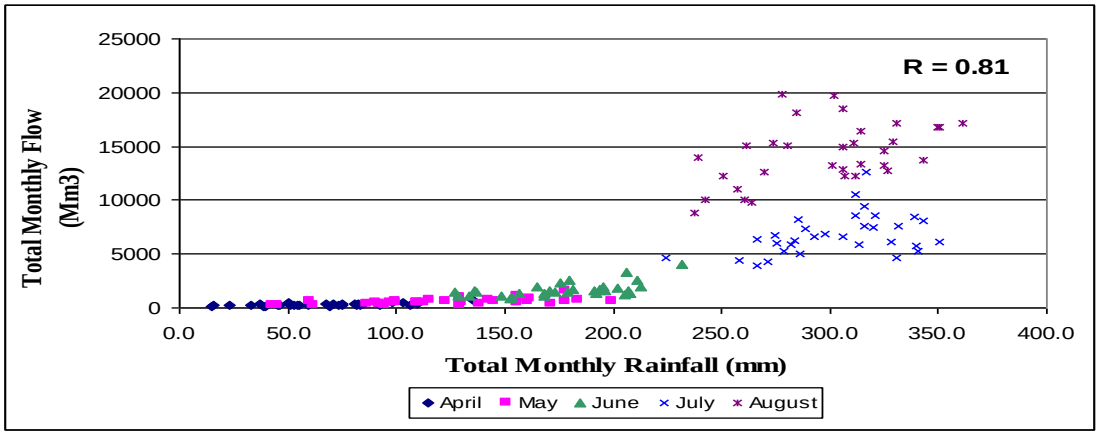

Figure 5: Scatter plot for rainfall-runoff relationship for rising stage data.

Table 2: Correlation coefficient results (R) for rising and falling stage months.

Flow	Rainfall Period/Month								
	Period	April	May	June	July	August	Sep	October	Period
April	Rising Stage	0.67							
May	0.81		0.55						
June				0.59					
July					0.47				
August						0.47			Falling Stage
Sep							0.58		
October								0.52	
November									0.92

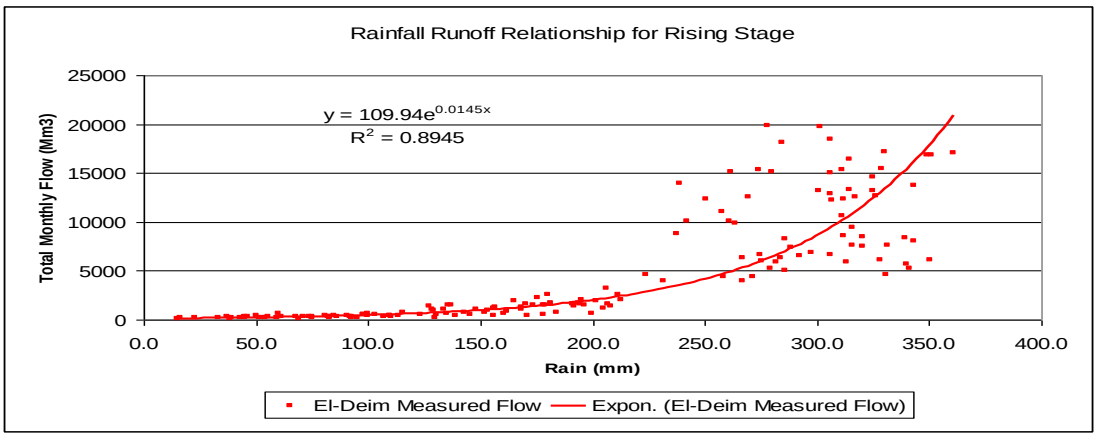

Figure 6: Scatter plot for rising stage data, and the best-fit line for the non-linear rainfall-runoff relationship. 1 mm of water depth is equivalent to 172.25 Mm^3 of water.

Relative prediction errors for the estimates from the previous equation are obtained and plotted as shown in figure 7. Equation 2 is used to calculate relative errors (%) from the predictions (F_t) based on the previous equation.

$$RE = 100 *(F_t - F_m)/F_m \quad (2)$$

Where F_m is the measured total monthly flow, F_t is the estimated total monthly flow, and RE is the percentage relative error. The figure reveals the tendency of the equation to over estimate the flows during the month of July and underestimation in August due to the nature of the exponential term in the equation. Otherwise the errors are well distributed during the remaining of the whole period. About 10% of the records have extreme relative errors of more than 80% during April, May, and July. Higher values for the relative errors during April and May are due to the decremented observations during the earlier period.

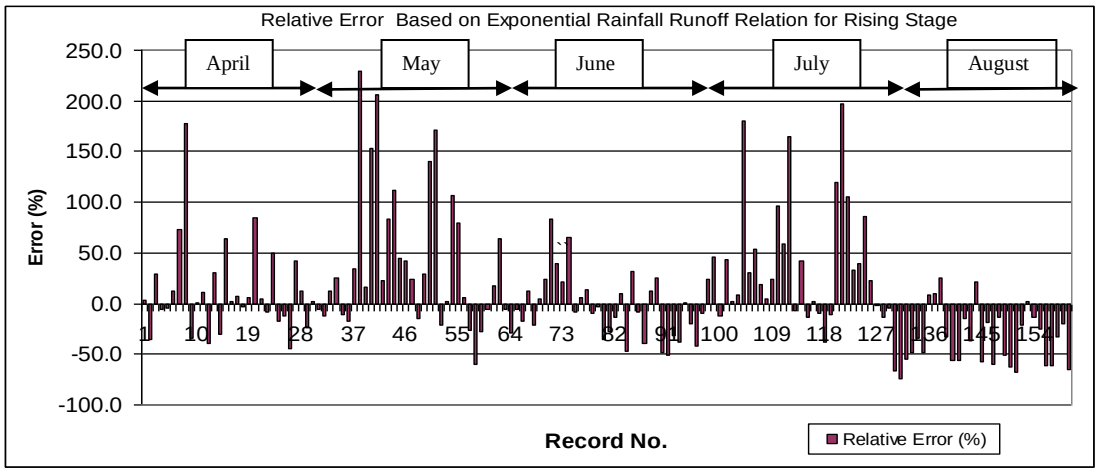

Figure 7: Relative prediction errors for the rising stage estimation.

4.2.2. Falling stage: Figure 8 shows the scatter plot and the regression line results (slope and intercept) for this case. In the analysis of the falling stage relationship, testing procedure was achieved by keeping away part of the data as hidden (a total of 24 random records for six years). Later on, results from the regression line were applied to the hidden data for verification.

As a result of the regression analysis, Equation 3 of the falling stage is given along with the corresponding coefficient of determination (R^2).

$$F_t = 2095.6 + 42.38 * R_t \quad , R^2 = 0.85 \qquad \text{For falling stage} \qquad (3)$$

Where in the above equation, F_t is the total monthly flow at month (t) in (Mm^3), and R_t is the total monthly rainfall in (mm). The intercept in the above equation represents physically the base flow term, whenever groundwater is the only contribution to stream flow, while there is no rainfall and therefore no contribution from the surface runoff. Regarding the regression line slope, common t-tests of significance at (1% error) concluded the significance of the equation.

Finally to address prediction errors from the previous equation, relative errors are calculated based on equation 2 and plotted. Figure 9 demonstrates the prediction errors' results. The figure shows that few records have absolute relative prediction errors of more than 80%. As shown in figure 9, four out of 128 records for this case were observed as extremes. The extreme errors observed in figure 9 are for some records during the months of November, while low flow observations are recorded during this month.

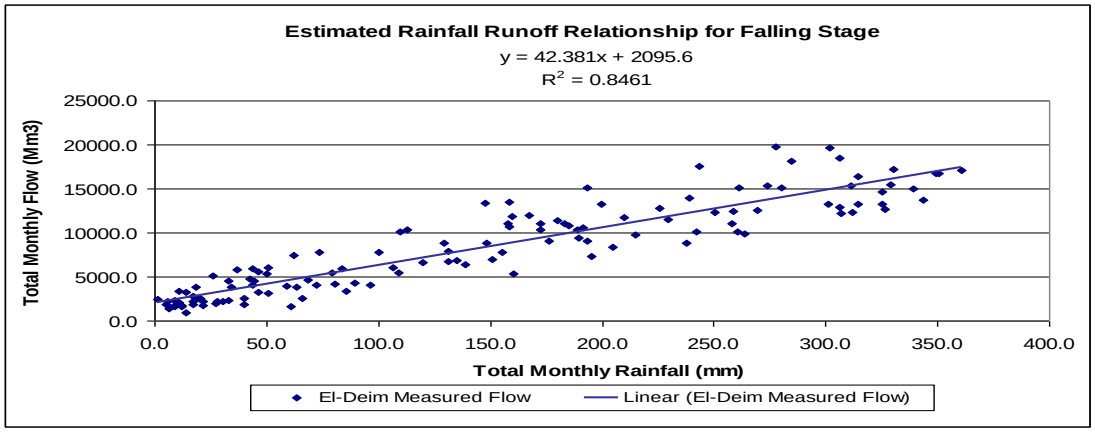

Figure 8: Scatter plot for falling stage data and the regression line for the rainfall-runoff relationship. 1 mm of water depth is equivalent to 172.25 Mm^3 of water.

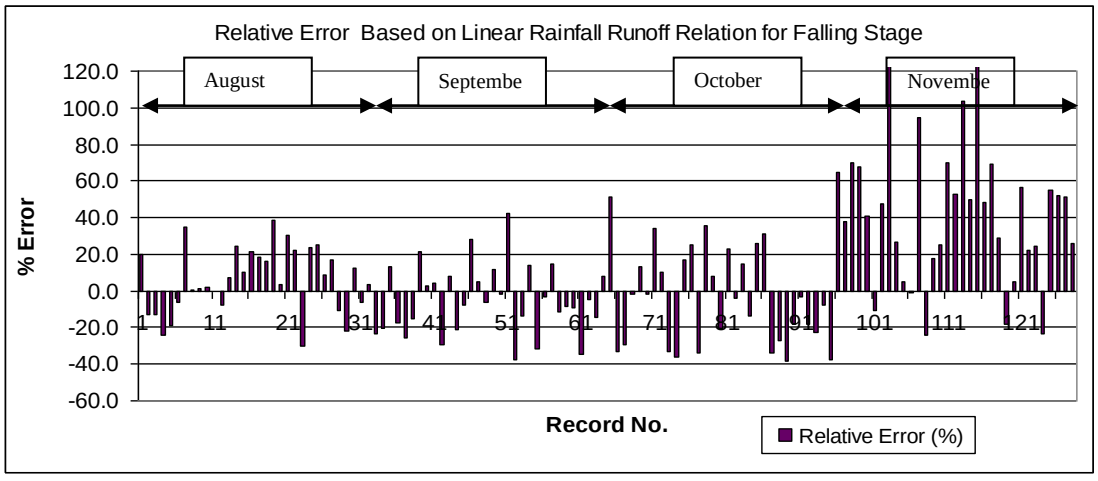

Figure 9: Relative prediction errors for the falling stage estimation.

5. DISCUSSIONS

The explanation of the physical phenomenon associated with the hysteresis loop in the current study is related to the progressive erosion/sedimentation processes driven by rainfall in the upper rivers catchments. While rainfall intensities start to increase during April and May (with maximum monthly potential evapo-transpiration in April), part of this rain is intercepted and collected in depression storage; meanwhile the rainfall energy is exploited in the erosion mechanism. Different forms of erosion (sheet, rill, gully, etc.) are formed and responsible of the increased friction forces during this period (rising stage). This explains the lower runoff (stream flow) during this period compared with the runoff during the falling stage period at the same monthly rainfall depths as shown in figure 4b.

Following the peak rainfall intensities during July and August (with minimum monthly potential evapo-transpiration in August), and during the falling stage of rainfall, the formed channels are filled up with water. Hence, water depth will build up and surface detention will increase causing friction forces to decrease, and therefore an increase in the stream flow. This again explains the higher stream flow during the falling period compared with its value during the rising stage period at the same monthly rainfall depths. This finding justified the decision made regarding the analysis of each stage separately.

Recalling figure 4b for the whole data plot, the regression results for the two stages can be presented along with the data on a separate figure. In additions, the previous findings presented in the form of Equations 1 and 3 (in volumetric units) are transformed to a different scale representing the catchment runoff in mm units. Given the shed area of the Abbay of 172,250 Km^2, the transformation factor is 1 mm of water depth to 172.25 Mm^3 of water. Dividing by the transformation factor, Equations 1 and 3 are rewritten in the following forms.

$RO_t = 12.08 + 0.25\ R_t$, $R^2 = 0.85$ For falling stage (4)

$RO_t = 0.64e^{0.015\mathbf{R}}t$, $R^2 = 0.895$ For rising stage (5)

Where in the above equations, RO_t and R_t are the runoff and rainfall at time (t) in mm units. Figure 10 demonstrates the final findings for the two stages (Equations 4 and 5) on the same scale along with the whole data. All marks in blue are for the months of falling stage period, while marks in red are for the months of rising stage period.

Regarding runoff coefficients, actual runoff coefficients are first obtained on monthly basis by dividing the runoff by the corresponding monthly rainfall based on the real two sets of measurements. Monthly runoff coefficients can be directly estimated from the previous equations by substituting monthly rainfall and dividing the equation's outcomes by the monthly rainfall. The runoff coefficients results along with the rainfall and runoff depths are shown in table 3. The table shows that the estimated runoff coefficients are matching the actual runoff coefficients

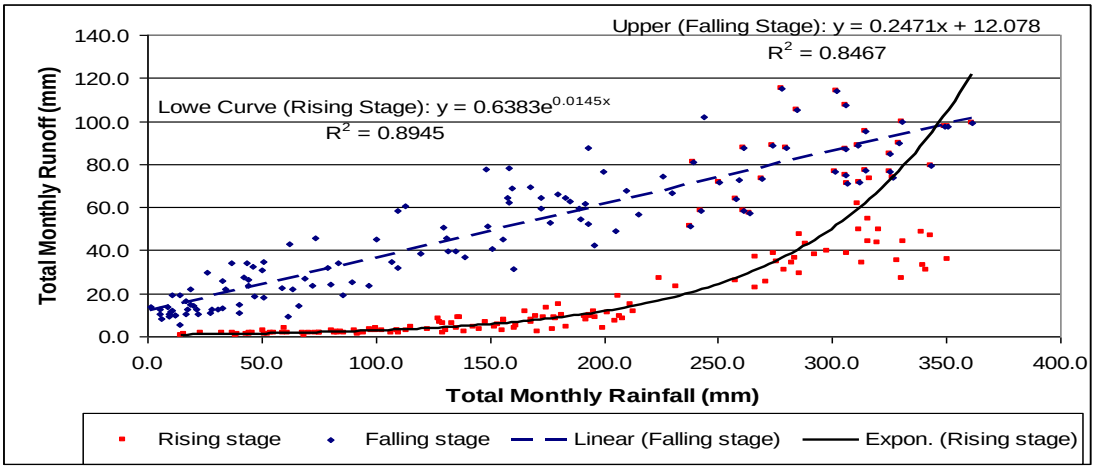

Figure 10: Scatter plot for the monthly rainfall-runoff data, showing both of the best-fit lines for rising stage and falling stage. 1 mm of water depth is equivalent to 172.25 Mm^3 of water.

Table 3: Average total monthly rainfall, actual and estimated runoff, and runoff coefficients.

Month	Avg. Rain (mm)	Runoff (mm)		Runoff Coefficient (%)	
		Estimated	Actual	Estimated	**Actual**
April	68.5	1.7	1.7	2.5	**2.5**
May	109.7	3.1	3.2	2.9	**2.9**
June	171.8	7.7	9.8	4.5	**5.7**
July	306.1	54.0	39.4	17.7	**12.9**
August	300.0	67.8	83.0	22.6	**27.7**
Sep	184.5	57.7	62.0	31.3	**33.6**
Oct	72.8	30.1	32.5	41.3	**44.6**
Nov	25.7	18.4	13.4	71.7	**52.1**
All season Avg.	**1239.3**	**240.7**	**245.0**	**19.4**	**19.7**

It is also clear from the figures in the table that during the recession period (August-November), rainfall depths are decreasing sharply from 300 mm to 25 mm compared to the decrease in the runoff from 68 mm to 18 mm, which makes the corresponding runoff coefficient are getting higher at the end of the period. Variations in the runoff coefficients are between 3 and 23% during the months of the rising stage (April- August); meanwhile it reaches 72% during November, which could be due to the contributions of other factors in the runoff such as the base flow and/or the evapo-transpiration. The overall seasonal runoff coefficient for the catchment during the study period is about 20%.

Findings of this study presented in Equations (1 and 3) were applied to check the validation of the estimated flow hydrographs for the period 2002-2005. Results of the estimated flow hydrographs for the period compared to the measurements are shown in figure 11. It is clear that the estimated flows are underestimating the measurements, but in general the whole patterns are matching each other. Results obtained using other forecasting tools such as the NFS by Elshamy (2008) also underestimated El-Diem measurements during earlier periods (1940-1955) and (1990-1994). Regarding the estimations of the peak flows in the current study, the estimates for the years 2002, 2003, and 2004 peak flows are underestimated by about 27-35%.

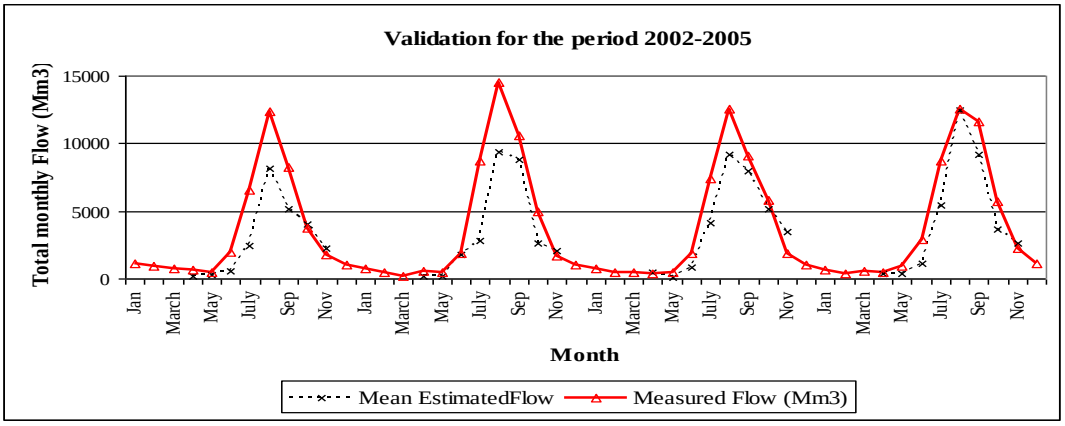

Figure 11: Validation results for the 2002-2005 estimated flow hydrographs.

6. CONCLUSIONS AND RECOMMENDATIONS

Hysteresis loop was observed in the rainfall-runoff relationship, which depicts the physical behavior and natural conditions in the uplands' streams and rivers. Due to this phenomenon, it was found that the runoff during the months of April and May (rising stage) are less than the runoff during October and November (falling stage) with the same rainfall depths. Meanwhile, runoff coefficients during October and November are much higher than their values during April and May, which could be due to the contribution of the base flow by the end of the rainy season in November. It was also found that the overall seasonal runoff coefficient for the catchment during the study period is about 20%.
The recommendations for further research are outlined as follows:

- Investigation of the lag-time between both of the rainfall and stream flow hydrographs and its impact on the results.
- Estimation of the 10-days mean/monthly runoff coefficients at the sub catchment level of the Abbay basin.
- Dissemination of the actual discharge measurements for the Abbay sub catchment gauge stations.

General recommendations are outlined as follows:

- Dissemination of daily rainfall data for the Eastern Nile Basin (ENB) countries between Ethiopia, Egypt and Sudan.
- Dissemination of the actual discharge measurements for the existing gauge stations and new proposed stations.

7. REFERENCES

1. WDS, (2014), *World Development Census*, World Bank web site. www.wb.org.
2. Negash, F., (2012), *Managing water for inclusion and sustainable growth in Ethiopia: Key challenges and priorities*, European Report on Development.
3. IPoE, (2013), *International Panel of Experts (IPoE) on Grand Ethiopian Renaissance Dam Project (GERDP)*, Unpublished report, May 2013.
4. Peggy, A.J. and D. Curtis., (1994), *Water balance of Blue Nile basin in Ethiopia*, Journal of Irrigation and Drainage Engineering, Vol. 120(3):573-590.
5. DICAM, (2011), *Flood frequency analysis at annual and seasonal scale for the Blue Nile River in Ethiopia (Research Contract between Studio Pietrangeli and DICAM)*, Final report, Universita degli Studi di Bologna, Italy, Nov. 2011.
6. King, A. M. (2013), *An Assessment of reservoir filling policies under a changing Climate for Ethiopia's Grand Renaissance Dam*, A Thesis Submitted to the Faculty Of Drexel University, May 2013.
7. Conway, D., (2000), *The Climate and Hydrology of the Upper Blue Nile River*, The Geographical Journal. Vol. 166(1): 49-62.
8. Abtew, W., A. M. Melese, and T. Dessalegne., (2008), *Characteristics of Monthly and Annual Rainfall of the Upper Blue Nile Basin*, Proceedings of the Workshop on Hydrology and Ecology of the Nile River Basin under Extreme Conditions. Addis Ababa, Ethiopia. June 16-19, 2008.
9. Bashar, K.E., F. Mutua, D.M.M. Mulungu, T. Deksyos, and A. Shamseldin., (2006), *Appraisal Study to select suitable Rainfall-Runoff model(s) for the Nile River Basin*, Proceedings of International Conference of UNESCO Flanders Friend/Nile Project, 12-15 Nov. 2005.
10. Elshamy, M.E., (2008), *Assessing the Hydrological Performance of the Nile Forecast System in Long Term Simulations*, Nile Water Science & Engineering Magazine. Vol. 1: 22-40, October 2008.
11. NCD, (2000), *Nile Basin Series of the Nile Control Department (NCD)*, The 14th Supplement, Volume IV, 2000.
12. Johnson, (1962), *Rain in East Africa*, Quart. J. Roy. Society.
13. Wilson E. M., (1983), *Engineering Hydrology*, English Language Book Society and Macmillan, third edition, 1983.
14. Zachary M. E., Selshi B. A., Tanmo S., Saliha A. H., Birhanu Z., Yilma S. and Kamaleddin E. B., (2012), *Hydrological processes in the Blue Nile, Published Book Section in* ***The Nile River Basin*** *Water, Agriculture, Governance and Livelihoods*, IWME, ILRI, CGIAR Program on Water and Food, 2012